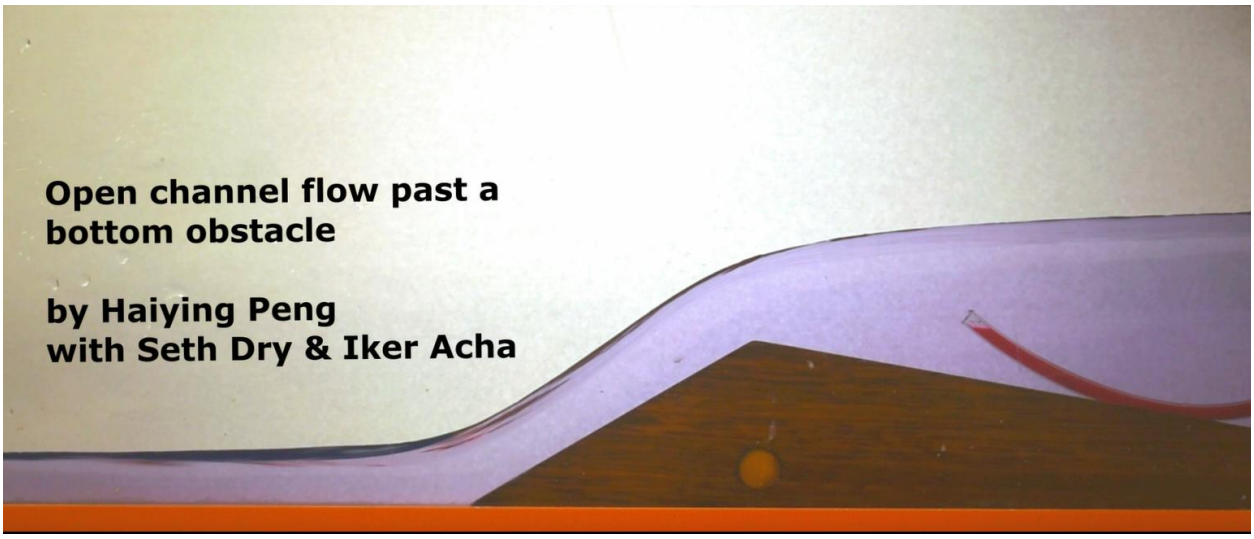

Team first report: Open Channel Flow Over a Low Triangular Obstacle in a Narrow Flume

Haiying Peng

MCEN 5151-002 Flow visualization

10/02/2025

1 Introduction

The purpose of this report is to describe and discuss the video on the cover. High-resolution versions of the video are available on flowvis.org, along with many other inspiring flow images and videos. This video was created for the Team First assignment in the MCEN 5151 Flow Visualization course in Fall 2025.

This video is intended to study open-channel flow over an obstacle. It shows open-channel flow in a flume moving from right to left, with red food dye injected as a tracer. Upstream of the obstacle, the water surface rises due to backwater effects. As the flow moves from right to left, the cross-section is reduced by the obstacle, and the velocity increases to pass over the crest. Downstream, the water surface drops sharply as the flow approaches near-critical conditions, where velocity increases and flow depth decreases.

The red dye clearly visualizes how the obstacle modifies the velocity distribution and the water surface profile. At the same time, the red dye adds color, aesthetic appeal, and even an element of interest, making the video less monotonous. This report documents and analyzes shallow free-surface flow in a narrow, recirculating flume, as water ascends a low triangular bump, crosses the crest, and accelerates down the lee face.

This report documents and analyzes shallow free-surface flow in a narrow, recirculating flume, as water ascends a low triangular bump, crosses the crest, and accelerates down the lee face. The objectives were to: (i) visualize drawdown and jet thinning, (ii) explain the observed features in terms of the competing roles of inertia, gravity, viscosity, and surface tension, and (iii) quantify the flow regime with nondimensional numbers (Froude, Reynolds, Weber/Bond) using measurements extracted from the video.

2 Methodology

2.1 Test setup

The experiment was conducted in a pump-driven recirculating flume. The dimensions of the flume are shown in Figure 1(a), and the dimensions of the triangular obstacle used are shown in Figure 1(b). The flume was not perfectly horizontal but had a slight slope, with a bed slope of approximately 0.5% (higher on the right, lower on the left).

During the experiment, the room temperature was about 22 °C. Because the water in the flume had been stored at this temperature for an extended period, the working fluid was assumed to be at approximately 22 °C. Accordingly, the density was taken as density ρ = 997.8kg/m3, the kinematic viscosity as ν = 9.57 * 10^-7 m2/s, and the surface tension as σ = 0.072 N/m.

(a)

(b)

Figure 1. Experimental setup: (a) Flume. (b) Obstacle.

2.2 Flow discussion

From the video, the following can be observed: as the flow approaches the obstacle, the free surface lowers while the flow accelerates up the slope. At the crest, the flow becomes shallow and fast, producing a thin, high-velocity jet. Beyond the crest, the flow does not return to a greater depth but instead develops into a sustained supercritical jet, consistent with the lack of sufficient tailwater depth to trigger a hydraulic jump.

The primary forces shaping this behavior are inertia and gravity. Viscosity is negligible at the bulk scale (though it sustains boundary layers), and surface tension plays no role except in generating small ripples.

To quantify these qualitative observations, the flow regime can be characterized by nondimensional parameters such as the Reynolds, Froude, and Weber numbers. These provide a framework to compare the relative importance of inertia, gravity, viscosity, and surface tension.

2.2.1 Preparation: Measurements Used for Calculations

1. local water depth

Upstream before the obstacle: $h_u = 9.81\ cm$

At the crest, water surface height =7.708cm; over-crest depth $h_c = 2.628\ cm$

Far downstream after clearing the obstacle: $h_d = 1.577\ cm$.

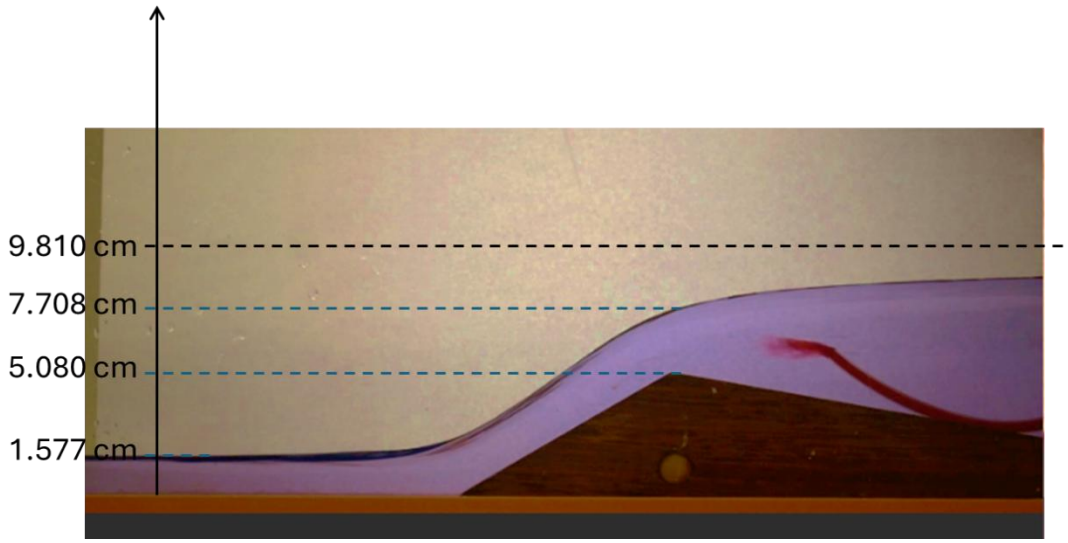

Figure 2. Local water depth

2. Flow Velocity

The approximate flow velocity at different stages was obtained by frame-by-frame observation, comparing the movement of injected food dye in the water. A reference image is provided in Figure A1 of the Appendix.

Upstream before obstacle: $U_u = 0.25\ m/s$,

Just before crest $U_{bc} = 0.425\ m/s$,

At crest $U_c = 0.945\ m/s$,

Early down $U_{ed} = 0.425\ m/s$,

Mid down $U_{md} = 0.796\ m/s$,

Late down $U_{ld} = 1.486\ m/s$.

For a rectangular, single-stream flow, the discharge per unit width, q = Uh, should be approximately constant.

q=Uc*hc=0.945×0.02628 ≈ 0.0248 m2/s.

Uld = q/hld ≈0.0248/0.01577≈1.57 m/s, very close to the estimated 1.486 m/s.

Because the crest and far-downstream values are mutually consistent, q = 0.0248m2/s was adopted as the best estimate of discharge. With the flume width b = 0.0762 m , the volumetric flow is

$$Q = qb = 0.0248 * 0.0762 = 1.89\ L/s$$

Upstream before obstacle: $U_u = 0.253\ m/s$, $h_u = 0.09810\ m$;

At the crest: $U_c = 0.945\ m/s$, $h_u = 0.02628\ m$;

Far downstream after clearing the obstacle: $U_u = 1.57\ m/s$, $h_u = 0.01577\ m$;

These values are used in the following calculations.

2.2.2 Nondimensional analysis

Dimensionless parameters are used to identify the flow regime and to compare it with classical theory. The Froude number (Fr), Reynolds number (Re) and Weber number (We), Bond number (Bo) were estimated as follows.

1. Froude number (Fr)

$$Fr = \frac{U}{\sqrt{gh}}$$

- Upstream: $Fr_u = \frac{0.253}{\sqrt{9.81*0.09810}} = 0.26\ (subcritical)$.
- At crest: $Fr_u = \frac{0.945}{\sqrt{9.81*0.2628}} = 1.86\ (supercritical)$
- Far downstream: $Fr_u = \frac{1.57}{\sqrt{9.81*0.01577}} = 4\ (strongly\ supercritical)$

2. Reynolds number (Re)

$$Re = \frac{Uh}{\nu}$$

Hydraulic-depth Reynolds number:

$$Re_h = \frac{Uh}{\nu} = \frac{q}{\nu}$$

Because q = Uh is constant, Re_h is nearly the same at all positions

$$Re_h = \frac{0.0248}{9.57 * 10^{-7}} = 2.59 * 10^4$$

Obstacle-scale Reynolds number:

$$Re_o = \frac{Uh_o}{\nu}, obstacle\ height\ h_o = \ 0.0508\ m$$

Upstream: $Re_{o\_u} = 1.34 * 10^4$.

At crest: $Re_{o\_c} = 5.01 * 10^4$

Far downstream: $Re_{o\_d} = 8.34 * 10^4$

The Reynolds numbers indicate that the open-channel flow is fully turbulent throughout. On the obstacle scale, turbulence is strong, with large eddies and a thin turbulent boundary layer expected.

3. Weber number and Bond number

$$We_h = \frac{\rho U^2 h}{\sigma}$$

At crest: $We_h = \frac{997.8 * 0.945^2 0.02628}{0.072} = 3.25 * 10^2$

$$Bo = \frac{\rho g h^2}{\sigma}$$

At crest: $Bo = \frac{997.8 * 9.81 * 0.02628^2}{0.072} = 94$

The results show that: $We_h \gg 1$, indicates that surface tension is negligible for bulk jet dynamics, while $Bo \gg 1$, shows that gravity and inertia dominate over surface tension.

The nondimensional analysis confirms that the flow regime is fully turbulent and governed primarily by inertia and gravity. Reynolds numbers at both the depth and obstacle scales indicate that viscous effects are negligible in controlling the bulk motion. The Froude numbers reveal a clear transition from subcritical conditions upstream (Fr < 1) to supercritical flow at the crest and downstream (Fr > 1), consistent with the observed drawdown and jet thinning. The large Weber and Bond numbers ($We_h \gg 1$, $Bo \gg 1$) demonstrate that surface tension does not affect the bulk jet dynamics, although it may influence small-scale ripples. Taken together, these nondimensional parameters establish that the observed flow is best described as a turbulent supercritical jet governed by inertia–gravity interactions.

Many studies have investigated open-channel flow. For example, Shademani et al.[1] used the Finite Volume Method (FVM) to numerically simulate air flowing through an equilateral triangular obstacle placed in a horizontal channel. Their study focused on the laminar regime at low Reynolds numbers (Re ≤ 38.03), analyzing streamlines, pressure fields, and drag coefficients as functions of Re. The results showed that at low Re, the flow remained symmetric with no significant separation. As Re increased, symmetric vortices formed downstream of the obstacle, and near the critical value of Re ≈ 38, asymmetric flow and wake instabilities began to appear. The present experiment also examines flow past a triangular obstacle in a channel, but with water rather than air. Although the flow regimes differ (Shademani[1] studied laminar flow at low Re, whereas the present experiment lies in the turbulent range at Re ~ 10^4 – 10^5), the comparison illustrates the transition: as Reynolds number increases, the flow evolves from symmetric, stable laminar motion to unstable, turbulent, and eventually supercritical states.

Dias and Vanden-Broeck[2] studied the free-surface profiles of open-channel flow over submerged triangular obstacles. Assuming inviscid, incompressible, steady, two-dimensional potential flow, they solved the governing equations numerically. Their results revealed two solution types: one with subcritical flow upstream and supercritical flow downstream (i.e., a critical transition at the obstacle), and another with both upstream and downstream supercritical flow. They further showed that varying the obstacle size leads to free-surface drawdown, thin jets, and limiting solutions with a 120° free-surface angle. Observations from the present experiment closely match their numerical results: the upstream flow is subcritical (Fr < 1), transitions at the obstacle crest, and becomes a sustained supercritical jet downstream (Fr ≫ 1). This theoretical study provides a direct mathematical model and physical interpretation for the drawdown, jet thinning, and sustained supercritical flow observed in the present experiment.

3 Visualization techniques

Illumination was provided by an LED clip lamp placed behind a sheet of white paper to produce uniform lighting. The dye clearly visualized how the obstacle modified the velocity distribution and the water surface profile. Videos were recorded with a Nikon D3400 digital

camera, using a short exposure time (1/640 s), a wide aperture (f/5.6), and a high ISO setting (1600). These parameters allowed transient flow features to be recorded sharply without motion blur.

4 Photographic techniques

The photographic setup was designed to capture fine structures in the fog flow with high contrast and sharp resolution. A Nikon D3500 DSLR camera equipped with an 18–55 mm f/3.5–5.6G lens was used. The lens was set to a focal length of 55 mm, with an aperture of f/5.6. A short exposure time of 1/640 s and a high ISO setting of 1600 allowed transient flow features to be recorded sharply without motion blur. The video was recorded at a frame rate of 59.94 frames per second.

Size of the field of view (FOV) calculated as:

$$FOV_{Width} = D \times \frac{W_{sensor}}{f} = 73.152 \times \frac{23.5}{55} = 31.26\ cm$$

$$FOV_{Height} = D \times \frac{H_{sensor}}{f} = 73.152 \times \frac{15.6}{55} = 20.75\ cm$$

Where: sensor size 23.5mm x 15.6mm (Nikon D3400 DSLR)

Focal length: 55 mm

Object distance (camera–flume): 2.4 ft =73.152 cm

The camera was positioned 2.4 feet (73.152 cm) from the plastic measuring cup, corresponding to a field of view of approximately 31.26 cm × 20.75 cm at the subject plane.

The original video was edited using Movavi software. The video was slowed down, and portions of the original frame were cropped to remove distracting elements. The brightness, contrast, and tone were adjusted. The original background audio was removed and replaced with background music, with copyright information included at the end of the video.

5 Conclusion

The video successfully captures the dynamics of shallow open-channel flow over a low triangular obstacle in a narrow recirculating flume. As the flow approaches the obstacle, the water surface clearly draws down and the velocity increases. At the crest, the flow forms a thin, fast jet, and downstream the water develops into a sustained supercritical jet. This behavior

confirms a transition from subcritical to supercritical conditions, in agreement with the nondimensional analysis showing Froude numbers rising from 0.26 upstream to nearly 4 downstream.

What makes this video compelling is not only the scientific demonstration of inertia–gravity–dominated flow but also the visual clarity with which these features are revealed. The red dye tracer highlights the streamline compression, acceleration, and jet formation with striking contrast.

Regarding the lighting of the photograph, one improvement could be to reposition one or more light sources behind the white paper sheet.

References:

[1] Shademani, Roya, et al. "Assessment of air flow over an equilateral triangular obstacle in a horizontal channel using FVM." J. Math. Sci. Appl 1.1 (2013): 12-16.

[2] Dias, Frrédéric, and Jean-Marc Vanden-Broeck. "Open channel flows with submerged obstructions." Journal of Fluid Mechanics 206 (1989): 155-170.

Appendix

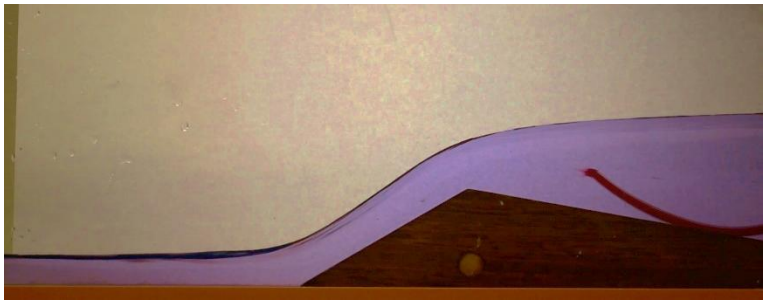

(a) 2.865s

(b) 2.932s

(c) 2.998s

(d) 3.031s

(e) 3.064s

(f) 3.097s

(g) 3.130s

Figure A1. The trajectory of food dye at different times, used to estimate the flow velocity of the liquid.